Supplement of The Cryosphere, 17, 1127–1149, 2023
https://doi.org/10.5194/tc-17-1127-2023-supplement

The Cryosphere Open Access EGU

Supplement of

Climatic control of the surface mass balance of the Patagonian Icefields

Tomás Carrasco-Escaff et al.

Correspondence to: Tomás Carrasco-Escaff (tcarrasco@dgf.uchile.cl)

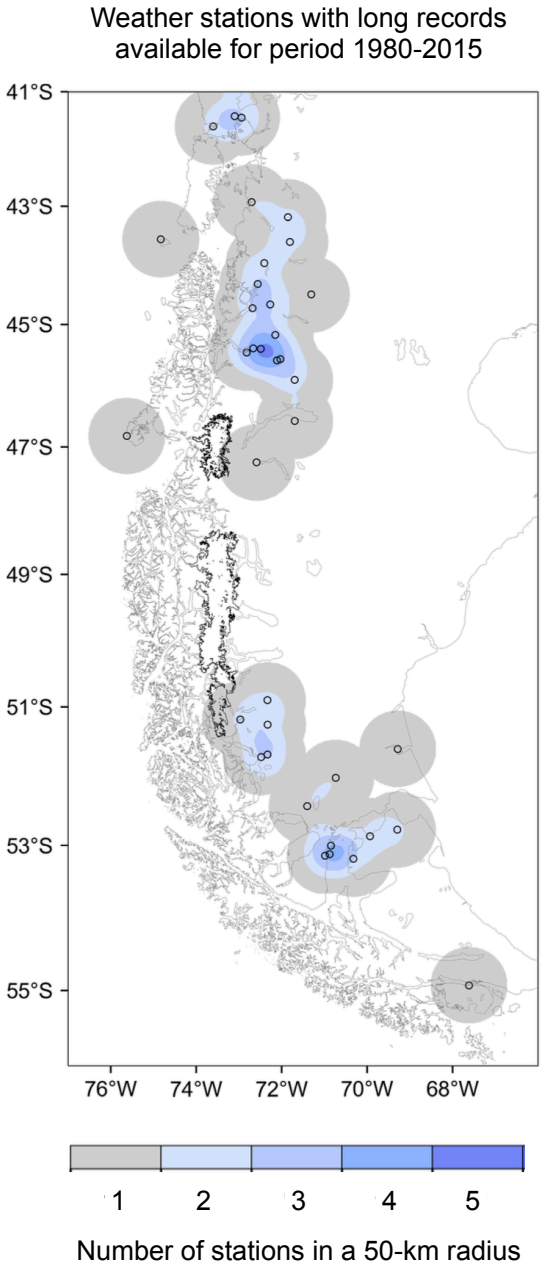

Figure S1. Heat map of weather stations with long records of precipitation measurements. Weather stations that register more than 75% of monthly precipitation data between 1980 and 2015 in Patagonia were used to construct the map. Colors indicate the number of stations with long records in a 50 km radius. Data were obtained from the Chilean Weather Service and the Chilean Water Agency.

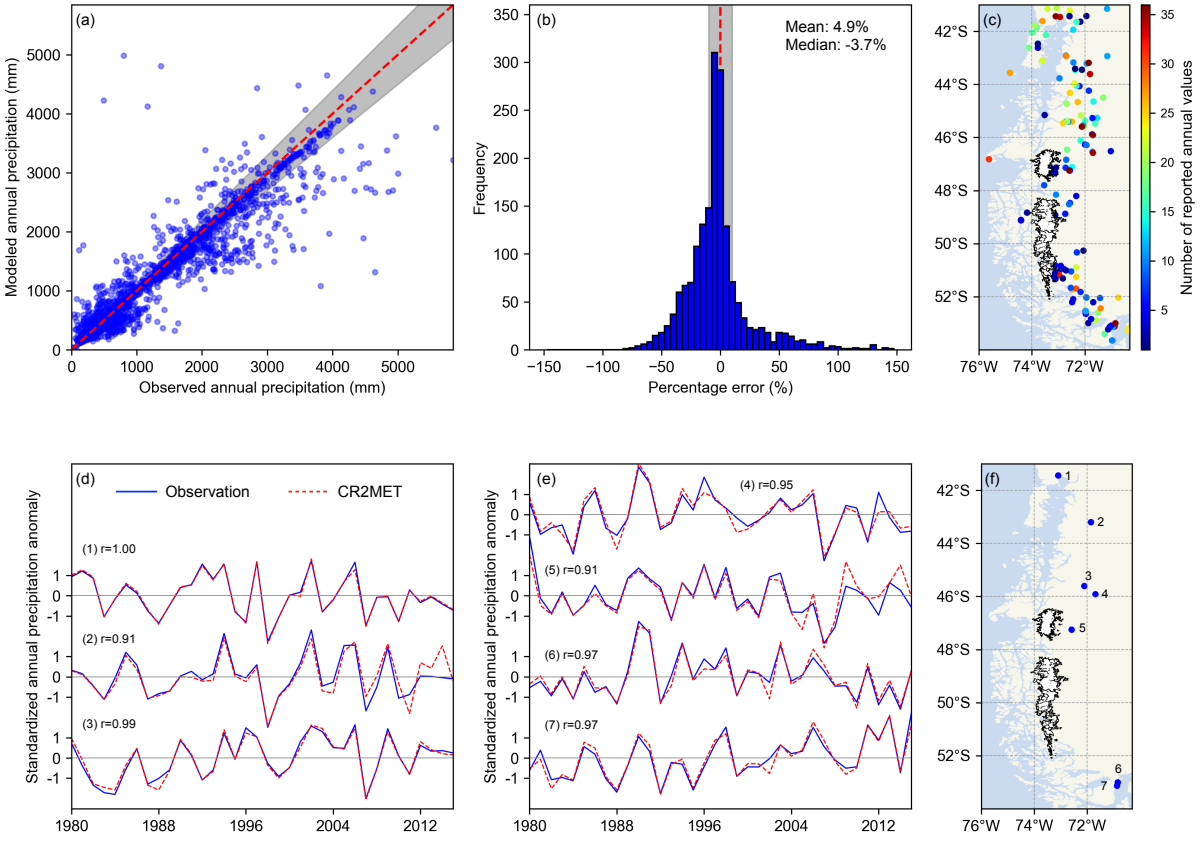

Figure S2. Evaluation of the CR2MET performance on annual precipitation estimation using the available surface weather stations. (a) Scatter plot of annual precipitation from the observations and corresponding CR2MET grid points (neares grid point). Each point represents available data of accumulated precipitation for years between 1980-2015 and weather stations located in Patagonia between 41-52º S. The segmented red line indicates no error in the estimation, while the grey area indicates an error ranging from -5% to 5% of the observed value. (b) Histogram of percentage errors of the CR2MET estimates. Each percentage error is calculated by subtracting the observed value from the CR2MET estimate and dividing it by the observed value. The grey area indicates an error ranging from -5% to 5% of the observed value. (c) Weather stations used in (a) and (b), along with their record lengths. (d) Time series of standardized anomalies of annual precipitation. Each blue line represents the observed annual time series obtained from a weather station located in Patagonia between 41-52º S with annual data for the full period 1980-2015. Segmented red lines correspond to the CR2MET estimates. Above each pair of lines is shown the station id and the correlation between the observed and CR2MET times series. (e) Continuation of (d). (f) Weather stations used in (d) and (e).

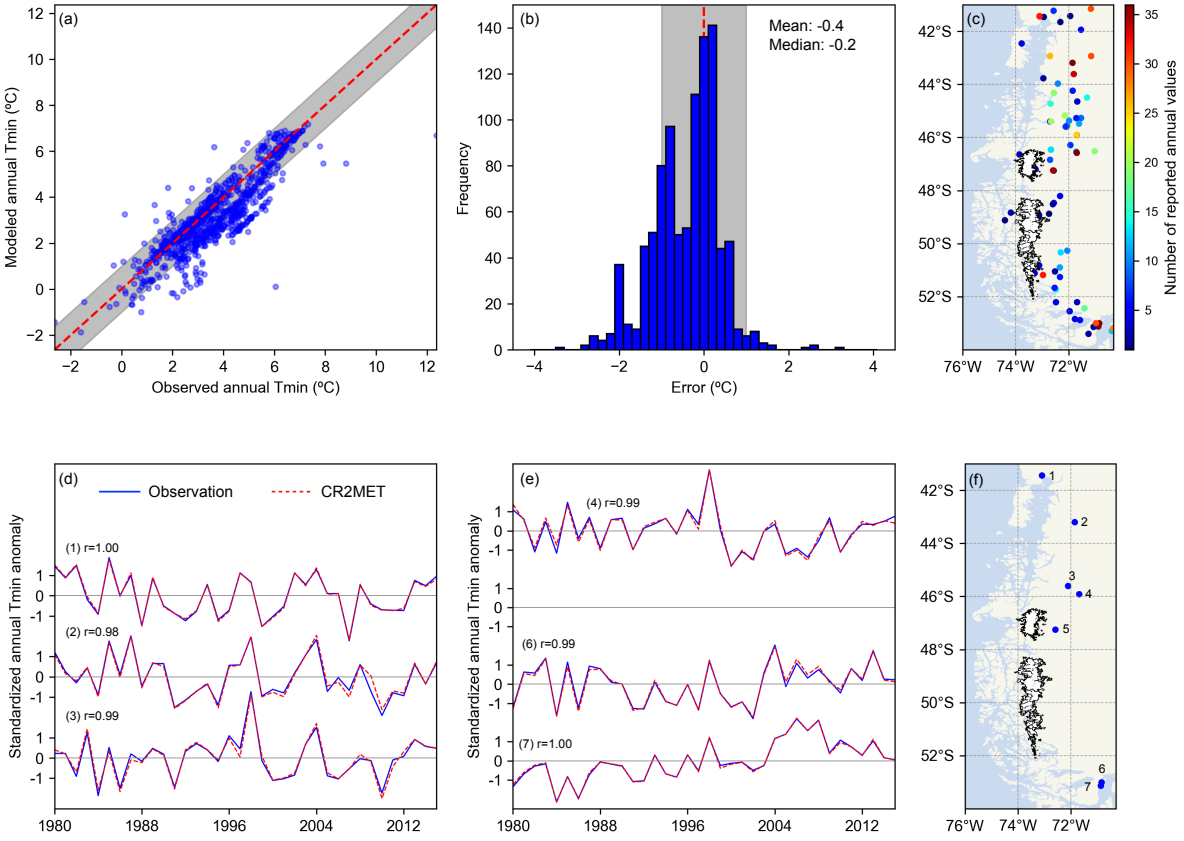

Figure S3. Evaluation of the CR2MET performance on the estimation of the annual mean of daily minimum temperature. (a) Scatter plot of annual mean of daily minimum temperature from the observations and corresponding CR2MET grid points (neares grid point). Each point represents available data of annual mean of daily minimum temperature for years between 1980-2015 and weather stations located in Patagonia between 41-52º S. The segmented red line indicates no error in the estimation, while the grey area indicates an error ranging from -5% to 5% of the observed value. (b) Histogram of errors of the CR2MET estimates. Each error is calculated by subtracting the observed value from the CR2MET estimate. The grey area indicates an error ranging from -5% to 5% of the observed value. (c) Weather stations used in (a) and (b), along with their record lengths. (d) Time series of standardized anomalies of the annual mean of daily minimum temperature. Each blue line represents the observed annual time series obtained from a weather station located in Patagonia between 41-52º S with annual data for the full period 1980-2015. Segmented red lines correspond to the CR2MET estimates. Above each pair of lines is shown the station id and the correlation between the observed and CR2MET times series. (e) Continuation of (d). (f) Weather stations used in (d) and (e).

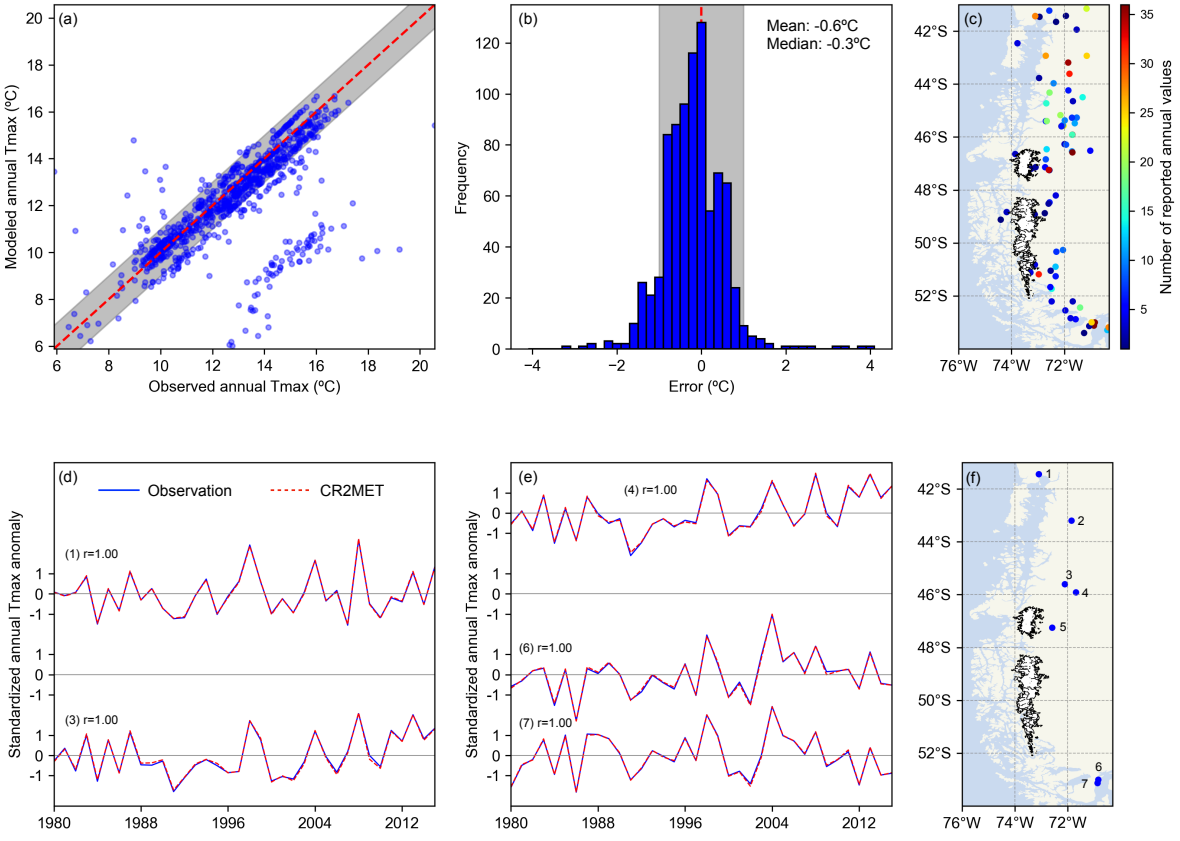

Figure S4. The same as in Fig. S3 but for the annual mean of daily maximum temperature.

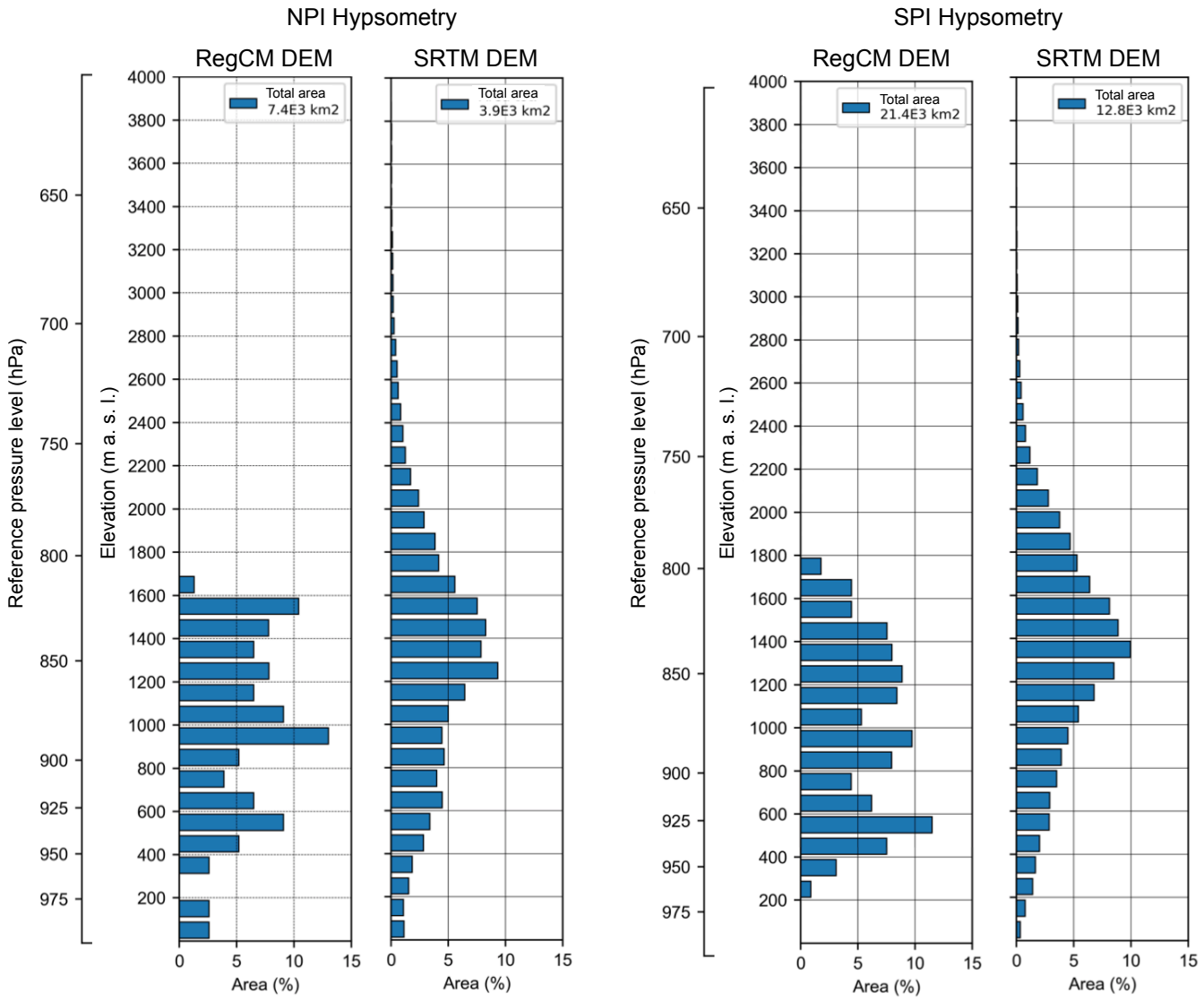

Figure S5. The two leftmost panels show the comparison between the NPI hypsometry obtained from the RegCMv4 DEM (∼10 km spatial resolution) versus the one obtained from the SRTMv3 DEM (∼90 m spatial resolution). The two rightmost panels show the same but for the SPI.

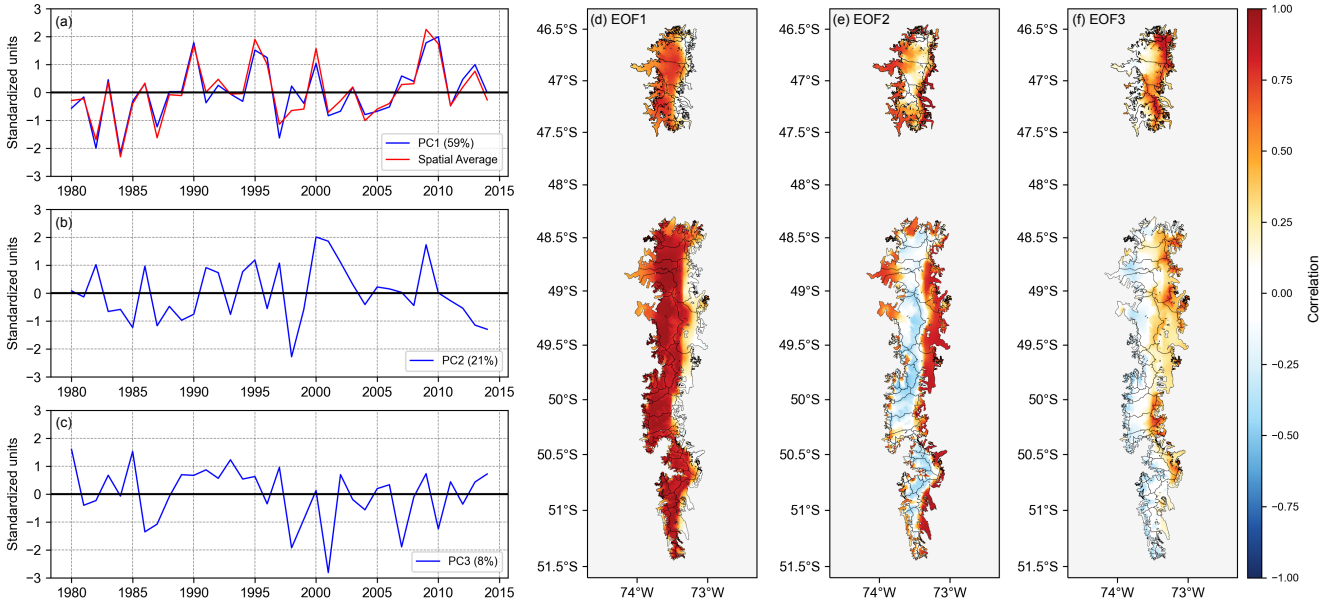

Figure S6. First three leading modes of variability of the annual SMB field of the Patagonian Icefields derived from the Empirical Orthogonal Function (EOF) analysis. (a) The blue line represents the first Principal Component (PC) scaled to unit variance (i.e., divided by the square-root of their eigenvalue), and the red line corresponds to the standardized anomalies of the spatial average of the annual SMB field over the Patagonian Icefields. (b) and (c): second and third PCs scaled to unit variance, respectively. (d) First EOF expressed as the correlation between the first PC and the time series of the annual SMB anomaly at each grid point. (e) and (f): the same as in (d) but for the second and third leading modes of variability, respectively.

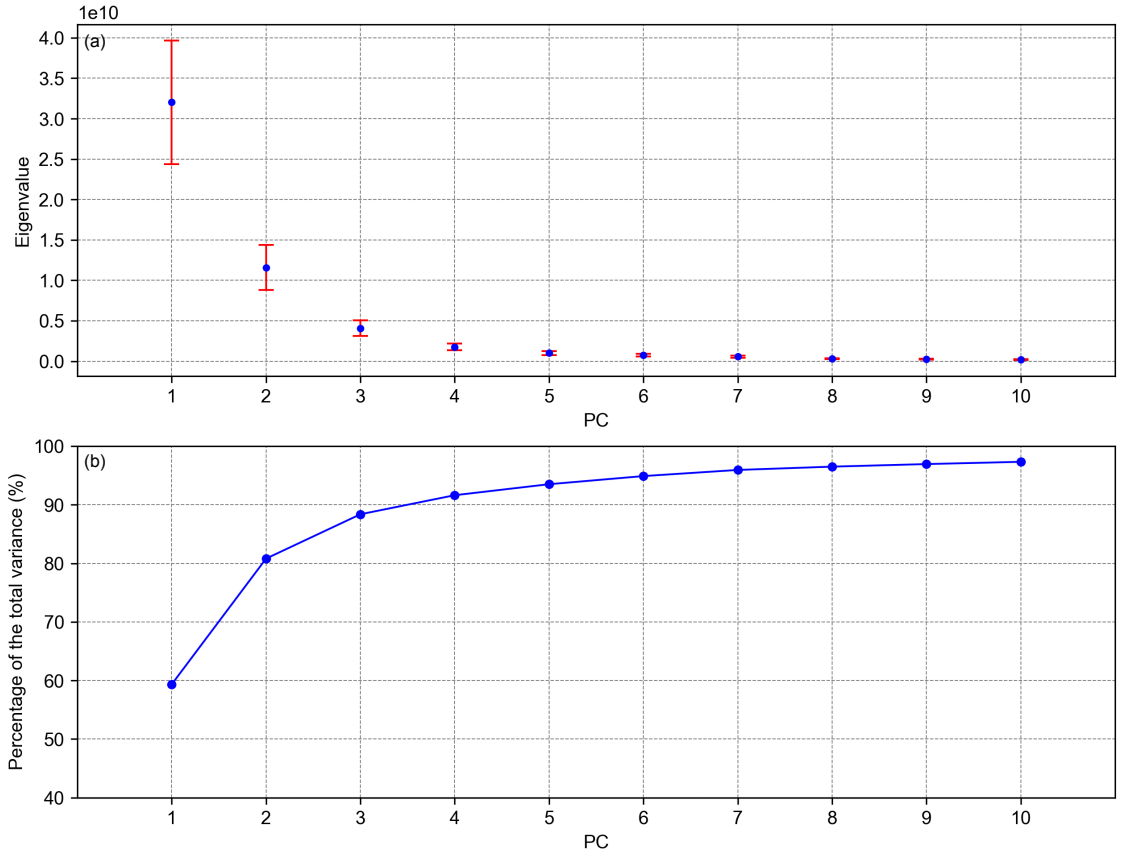

Figure S7. (a) Eigenvalues of the first ten leading modes of variability of the annual SMB field of the Patagonian Icefields derived from the EOF analysis (blue points) along with its typical errors (red error bars) computed using the method of North et al. (1982). (b) Accumulated percentage of the total variance explained by each PC.

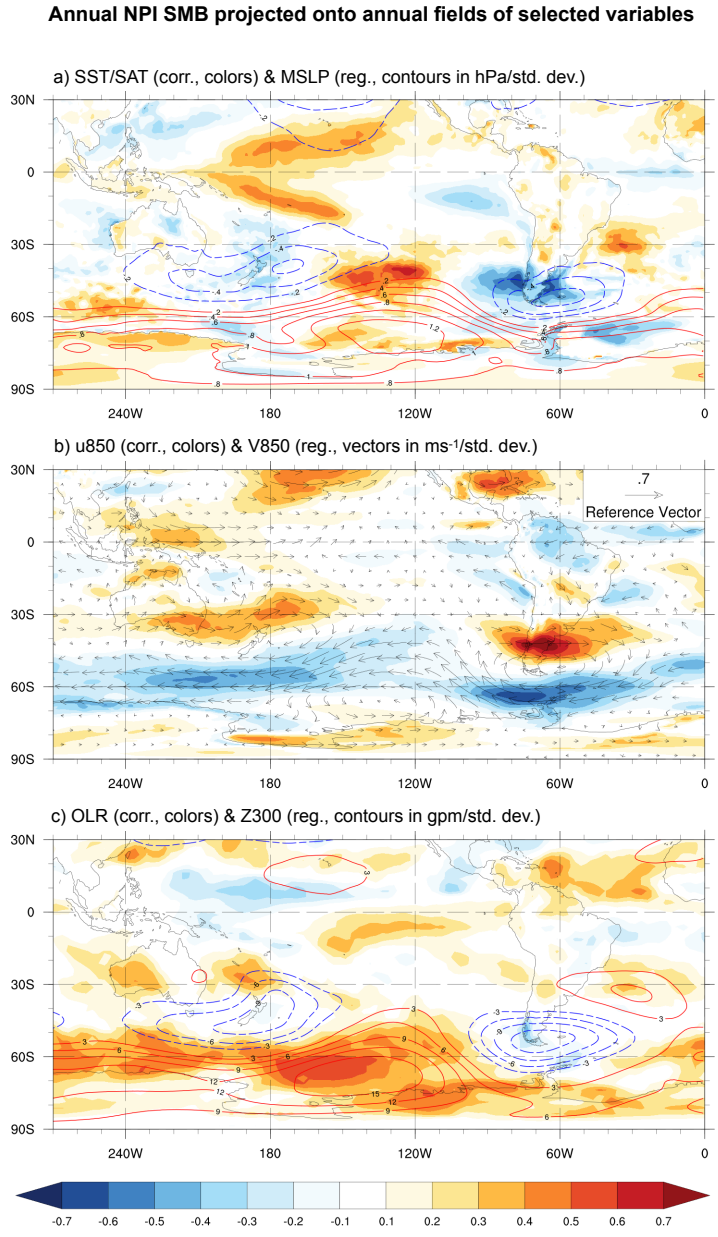

Figure S8. The same as in Fig. 8 in the main text but for the NPI-only annual SMB time series.

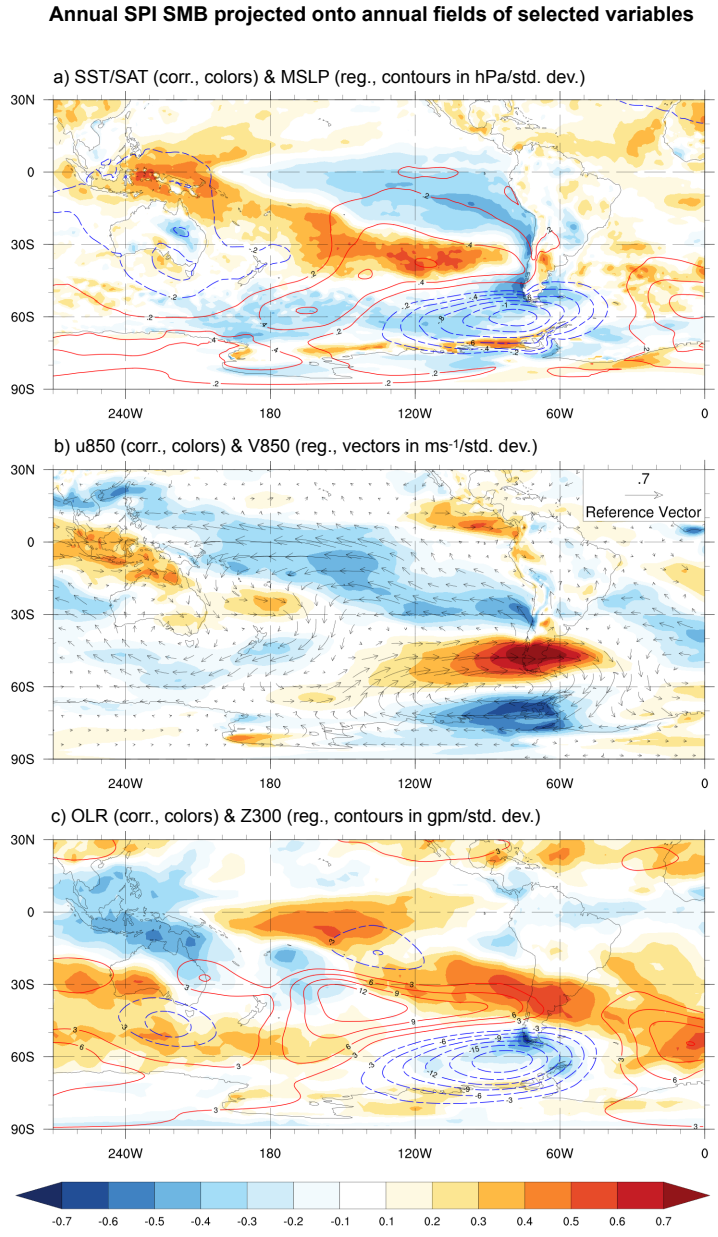

Figure S9. The same as in Fig. 8 in the main text but for the SPI-only annual SMB time series.

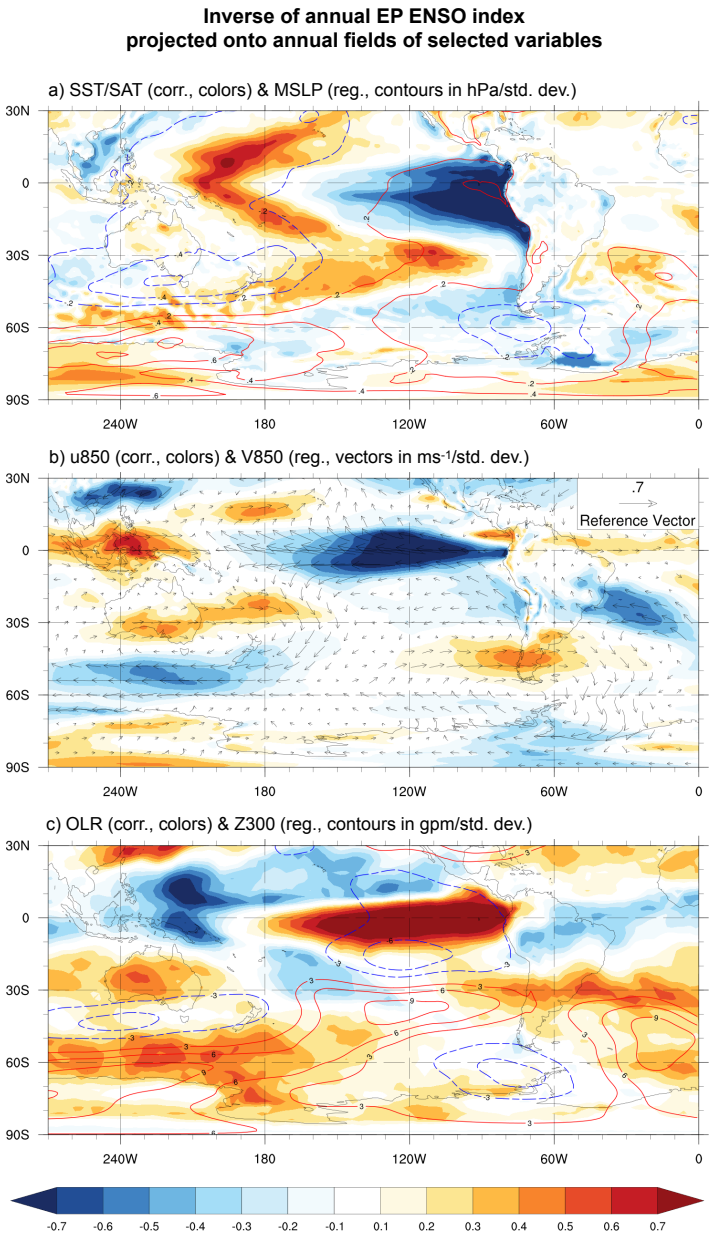

Figure S10. The same as in Fig. 8 in the main text but for the inverse of the annual EP ENSO index.

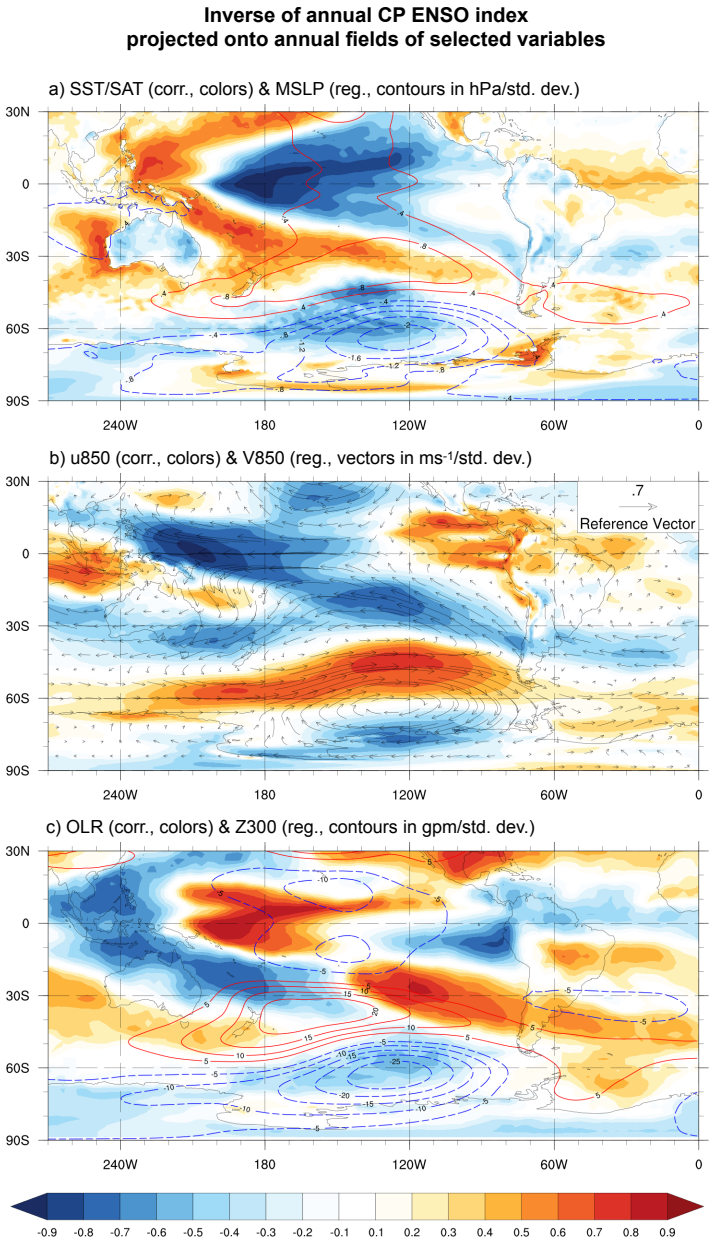

Figure S11. The same as in Fig. 8 in the main text but for the inverse of the annual CP ENSO index.

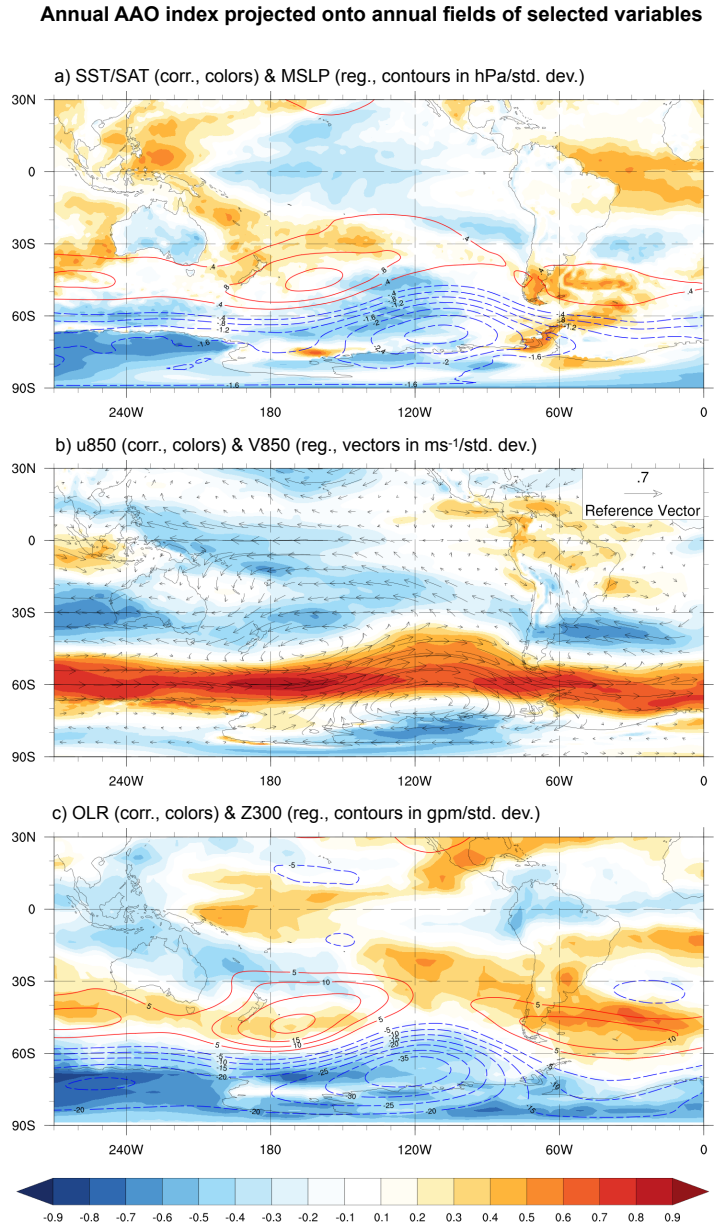

Figure S12. The same as in Fig. 8 in the main text but for the annual AAO index.

Table S1. Mean values of the annual (April to March), winter (April to September) and summer (October to March) time series of the spatially averaged modeled fields from 1980 to 2015.

Mean values	SMB	Accumulation	Ablation	Precipitation	Temperature	Insolation
Units	mm w.e.	mm w.e.	mm w.e.	mm w.e.	ºC	Wm^{-2}
Annual	469	4748	4279	6430	-1.82	123
Winter	1806	2633	827	3214	-3.44	56
Summer	-1336	2115	3452	3217	-0.20	191

Table S2. Standard deviations of the annual (April to March), winter (April to September) and summer (October to March) time series of the spatially averaged modeled fields from 1980 to 2015.

Standard deviation	SMB	Accumulation	Ablation	Precipitation	Temperature	Insolation
Units	mm w.e.	mm w.e.	mm w.e.	mm w.e.	ºC	Wm^{-2}
Annual	537	403	272	536	0.37	4
Winter	331	333	112	425	0.57	3
Summer	428	237	238	327	0.42	7

Table S3. Correlation between pairs of annual (April to March) time series of the spatially averaged modeled fields from 1980 to 2015. (*) Statistically significant value at a significance level of 5%.

Annual corr.	SMB	Accumulation	Ablation	Precipitation	Temperature	Insolation
SMB	1.00	-	-	-	-	-
Accumulation	0.87^{*}	1.00	-	-	-	-
Ablation	-0.68^{*}	-0.23	1.00	-	-	-
Precipitation	0.69^{*}	0.90^{*}	-0.02	1.00	-	-
Temperature	-0.25	0.19	0.78^{*}	0.45^{*}	1.00	-
Insolation	-0.44^{*}	-0.33	0.37^{*}	-0.53^{*}	-0.19	1.00

Table S4. Correlation between pairs of winter (April to September) time series of the spatially averaged modeled fields from 1980 to 2015. (*) Statistically significant value at a significance level of 5%.

Winter corr.	SMB	Accumulation	Ablation	Precipitation	Temperature	Insolation
SMB	1.00	-	-	-	-	-
Accumulation	0.94^*	1.00	-	-	-	-
Ablation	-0.15	0.18	1.00	-	-	-
Precipitation	0.86^*	0.97^*	0.32	1.00	-	-
Temperature	0.18	0.46^*	0.84^*	0.61^*	1.00	-
Insolation	-0.57^*	-0.59^*	-0.05	-0.66^*	-0.48^*	1.00

Table S5. Correlation between pairs of summer (October to March) time series of the spatially averaged modeled fields from 1980 to 2015. (*) Statistically significant value at a significance level of 5%.

Summer corr.	SMB	Accumulation	Ablation	Precipitation	Temperature	Insolation
SMB	1.00	-	-	-	-	-
Accumulation	0.90^*	1.00	-	-	-	-
Ablation	-0.90^*	-0.62^*	1.00	-	-	-
Precipitation	0.64^*	0.83^*	-0.31	1.00	-	-
Temperature	-0.70^*	-0.40^*	0.86^*	0.05^*	1.00	-
Insolation	-0.61^*	-0.58^*	0.51^*	-0.76^*	0.08	1.00

Table S6. Sensitivity of the modeled SMB to the main model parameters and to the complexity of the solar radiation remapping. $\overline{x}$ and s are the mean value and standard deviation (measured in mm w.e.) of the annual SMB time series obtained from each experiment, respectively. $\overline{x_0}$ and s_0 correspond to the same statistics but for the control time series. r represents the correlation between the annual SMB time series obtained from each experiment and the control time series.

Parameter	Value	$\overline{x}$	s	$\overline{x}-\overline{x_0}$	s/s_0	r
Δc_0 ($\mathrm{Wm^{-2}}$)	-4.0	758	532	289	0.99	1.00
	-3.0	687	533	218	0.99	1.00
	-2.0	615	534	146	1.00	1.00
	-1.0	543	535	73	1.00	1.00
	1.0	395	538	-74	1.00	1.00
	2.0	320	539	-149	1.00	1.00
	3.0	244	540	-225	1.01	1.00
	4.0	168	541	-302	1.01	1.00
Δc_1 ($\mathrm{Wm^{-2}{}^{o}C^{-1}}$)	-2.0	535	523	65	0.98	1.00
	-1.5	523	527	53	0.98	1.00
	-1.0	508	530	38	0.99	1.00
	-0.5	490	533	20	0.99	1.00
	0.5	447	540	-23	1.01	1.00
	1.0	422	544	-47	1.01	1.00
	1.5	395	547	-74	1.02	1.00
	2.0	367	551	-102	1.03	1.00
Albedo	A1	-714	561	-1183	1.05	1.00
	A2	-3436	620	-3905	1.16	0.98
ΔT_{th} (ºC)	-1.00	127	534	-342	0.99	1.00
	-0.75	217	534	-253	1.00	1.00
	-0.50	304	535	-166	1.00	1.00
	-0.25	388	536	-81	1.00	1.00
	0.25	548	537	79	1.00	1.00
	0.50	624	538	154	1.00	1.00
	0.75	697	539	227	1.00	1.00
	1.00	767	540	297	1.01	1.00
Sloped surface	/	850	415	1374	0.80	0.99

Table S7. The same as in Table S6 but for the sensitivity of the modeled SMB to the mean value of the near-surface air temperature and precipitation forcing.

ΔT	P_0	$\overline{x}$	s	$\overline{x} - \overline{x_0}$	s/s_0	r
-1.5	0.8	1078	465	608	0.87	0.99
-1.5	0.9	1688	501	1218	0.93	0.98
-1.5	1.0	2289	539	1820	1.00	0.98
-1.5	1.1	2884	577	2415	1.08	0.97
-1.5	1.2	3473	616	3004	1.15	0.97
-1.0	0.8	559	467	90	0.87	0.99
-1.0	0.9	1152	502	682	0.93	0.99
-1.0	1.0	1736	537	1266	1.00	0.99
-1.0	1.1	2313	574	1844	1.07	0.99
-1.0	1.2	2884	612	2415	1.14	0.98
-0.5	0.8	-8	470	-477	0.88	1.00
-0.5	0.9	565	502	96	0.94	1.00
-0.5	1.0	1129	536	660	1.00	1.00
-0.5	1.1	1685	571	1216	1.06	0.99
-0.5	1.2	2236	607	1767	1.13	0.99
0.0	0.8	-624	476	-1093	0.89	1.00
0.0	0.9	-72	505	-541	0.94	1.00
0.0	1.1	1003	570	534	1.06	1.00
0.0	1.2	1530	603	1061	1.12	1.00
0.5	0.8	-1291	485	-1760	0.90	0.99
0.5	0.9	-760	511	-1229	0.95	0.99
0.5	1.0	-242	540	-711	1.01	1.00
0.5	1.1	267	570	-202	1.06	1.00
0.5	1.2	770	602	300	1.12	1.00
1.0	0.8	-2012	502	-2481	0.93	0.98
1.0	0.9	-1501	523	-1970	0.98	0.98
1.0	1.0	-1005	548	-1474	1.02	0.99
1.0	1.1	-519	575	-989	1.07	0.99
1.0	1.2	-42	603	-512	1.12	0.99
1.5	0.8	-2790	524	-3259	0.98	0.96
1.5	0.9	-2296	542	-2765	1.01	0.97
1.5	1.0	-1820	563	-2289	1.05	0.97
1.5	1.1	-1357	586	-1826	1.09	0.98
1.5	1.2	-904	611	-1374	1.14	0.98

Table S8. The same as in Table S6 but for the sensitivity of the modeled SMB to the mean value of the surface downward solar radiation forcing.

R_0	$\overline{x}$	s	$\overline{x} - \overline{x_0}$	s/s_0	r
1.1	129	550	-340	1.03	1.00
1.2	-220	565	-690	1.05	1.00
1.3	-580	580	-1048	1.08	1.00
1.4	-948	596	-1418	1.11	1.00
1.5	-1326	613	-1795	1.14	0.99

Table S9. The same as in Table S6 but for the sensitivity of the modeled SMB to the interannual variability of the meteorological input. R^2 corresponds to the squared correlation.

Variability $\tau \geq 1$ yr removed from	Time series	$\overline{x}$	s	$\overline{x} - \overline{x_0}$	s/s_0	r	R^2
Precipitation	Annual	751	402	282	0.75	0.51	26 %
	Winter	1981	189	175	0.57	0.04	0 %
	Summer	-1230	334	107	0.78	0.82	67 %
Temperature	Annual	1225	561	756	1.05	0.67	45 %
	Winter	2208	417	402	1.26	0.86	74%
	Summer	-983	316	353	0.74	0.63	40 %
Insolation	Annual	479	510	9	0.95	0.98	95 %
	Winter	1806	319	0	0.96	1.00	99 %
	Summer	-1327	384	9	0.9	0.97	95 %